PNAS
www.pnas.org

Supplementary Information for

Structural insights into a dimeric Psb27-photosystem II complex from a cyanobacterium *Thermosynechococcus vulcanus*

Guoqiang Huang[a, 1], Yanan Xiao[b, c, 1], Xiong Pi[a, 1], Liang Zhao[a], Qingjun Zhu[b, c], Wenda Wang[b], Tingyun Kuang[b], Guangye Han[b, 2], Sen-Fang Sui[a, d, 2], Jian-Ren Shen[b, e, 2]

[a]State Key Laboratory of Membrane Biology, Beijing Advanced Innovation Center for Structural Biology & Frontier Research Center for Biological Structure, School of Life Sciences, Tsinghua University, Beijing 100084, China.
[b]Photosynthesis Research Center, Key Laboratory of Photobiology, Institute of Botany, the Chinese Academy of Sciences, Beijing 100093, China.
[c]University of Chinese Academy of Sciences, Yuquan Road, Shijingshan District, Beijing 100049, China.
[d]Department of Biology, Southern University of Science and Technology, Shenzhen, Guangdong 518055, China
[e]Research Institute for Interdisciplinary Science and Graduate School of Natural Science and Technology, Okayama University, Okayama 700-8530, Japan.

[1]These authors contributed equally to this work.

[2]Corresponding authors.
E-mails: hanguangye@ibcas.ac.cn or suisf@mail.tsinghua.edu.cn or shen@cc.okayama-u.ac.jp.

This PDF file includes:

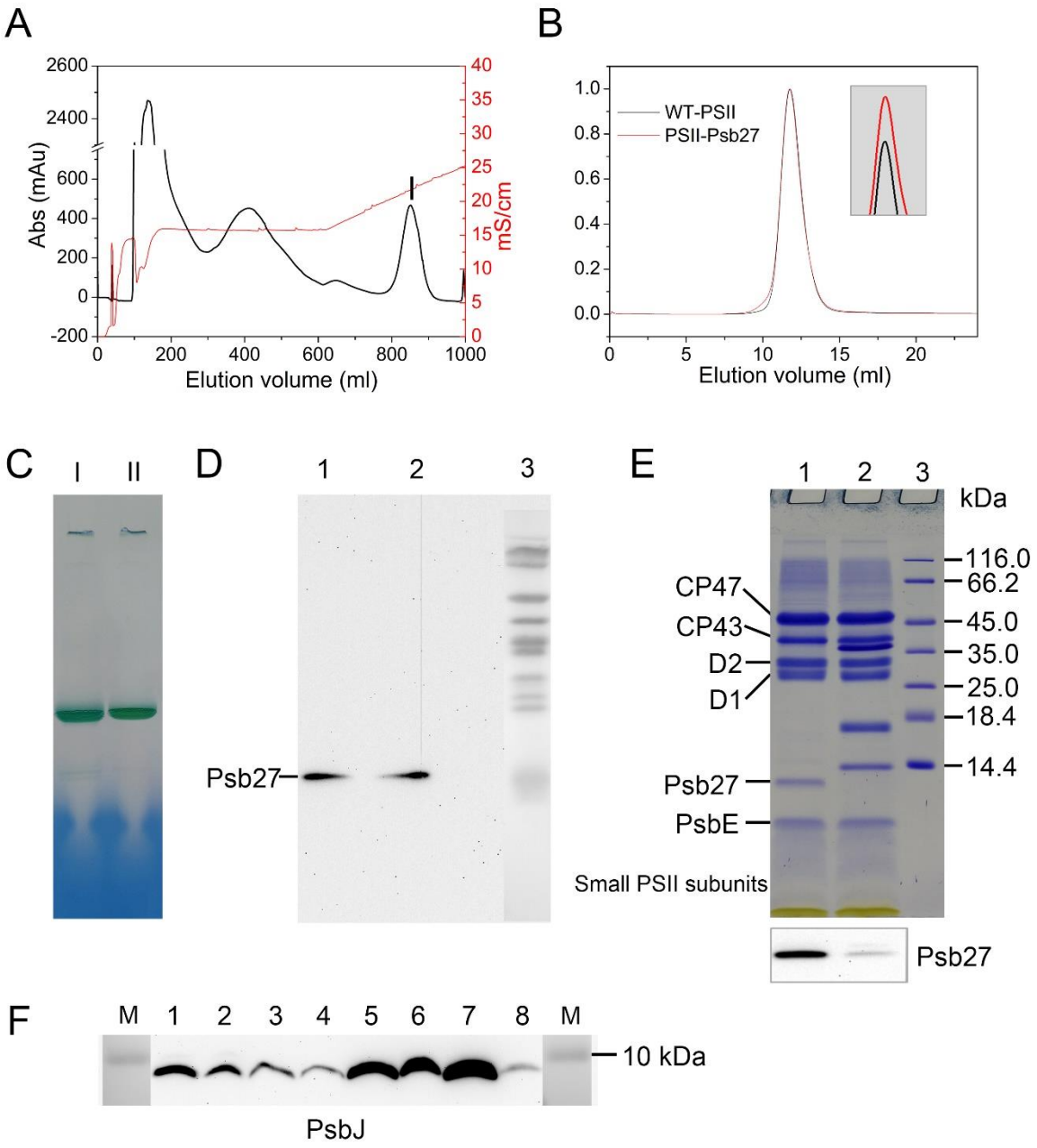

Fig. S1. Purification and characterization of the Psb27-PSII complex from the Δ*psbV* mutant of *T. vulcanus*. **A:** Elution pattern of the Psb27-PSII complex from a Q-Sepharose High-Performance anion-exchange column. Fraction labeled with a vertical bar was the dimer of Psb27-PSII, and was collected and used for single particle analysis in this study. **B:** Elution profile of the Psb27-PSII and native PSII dimer complexes from a size-exclusion chromatography. The column was eluted at a flow rate of 0.200 mL min^{-1} at 4°C and monitored by absorption at 280 nm. The results showed that the purified Psb27-PSII gave rise to a single peak, indicating that it is homogeneous in terms of its size. The elution peak was located at a very similar position as that of the native PSII dimer (see the insert), indicating that the Psb27-PSII obtained is also a dimer. **C:** BN-PAGE analysis of the purified Psb27-PSII complex after the size-exclusion chromatography. Lane I, Psb27-PSII; Lane II, native PSII dimer. **D:** Western-blotting analysis of the Psb27 in gels obtained by BN-PAGE and two-dimensional gel electrophoresis from Psb27-PSII sample before (lane 1) and after (lane 2) cryo treatment with liquid N_2, respectively, and lane 3 represents a molecular

weight marker. The Psb27 was detected with antibodies raised against Psb27 protein. The result shows that Psb27 is still associated with the dimeric complex even after the freeze-thaw treatment. **E:** SDS-PAGE analysis of the purified Psb27-PSII from *T. vulcanus*. Western-blotting analysis of Psb27 was shown in the bottom of the SDS-PAGE. Lane 1, Psb27-PSII; Lane 2, native PSII; Lane 3, marker. **F:** Western-blotting analysis of PsbJ during the process of Psb27-PSII purification from mutant and wild type (WT) cells of *T. vulcanus*. Western-blotting with an antibody raised against the PsbJ protein was shown. Lane 1, Lane 3, Lane 5, and Lane 7 are cells, thylakoid membrane, crude-PSII and PSII of WT cells, respectively. Lane 2, Lane 4, Lane 6, and Lane 8 are cells, thylakoid membrane, crude-PSII and PSII of the Δ*psbV* mutant cells. Lane M, marker.

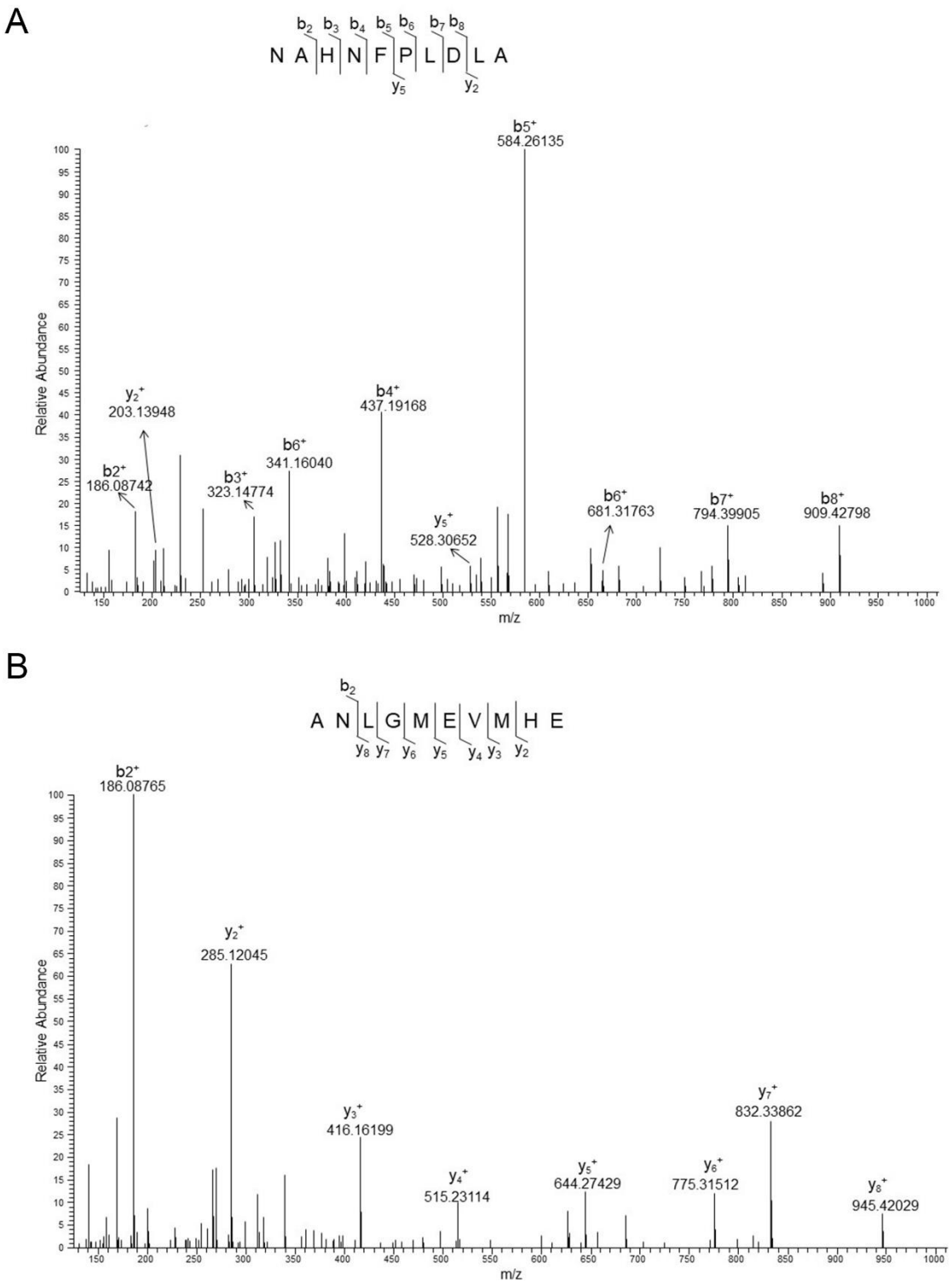

Fig. S2. Typical MS/MS spectra of the peptides from the D1 protein in the purified Psb27-PSII sample. Two types of C-terminal sequences were detected; one is NAHNFPLDLA (**A**) and the other one is ANLGMEVMHE (**B**).

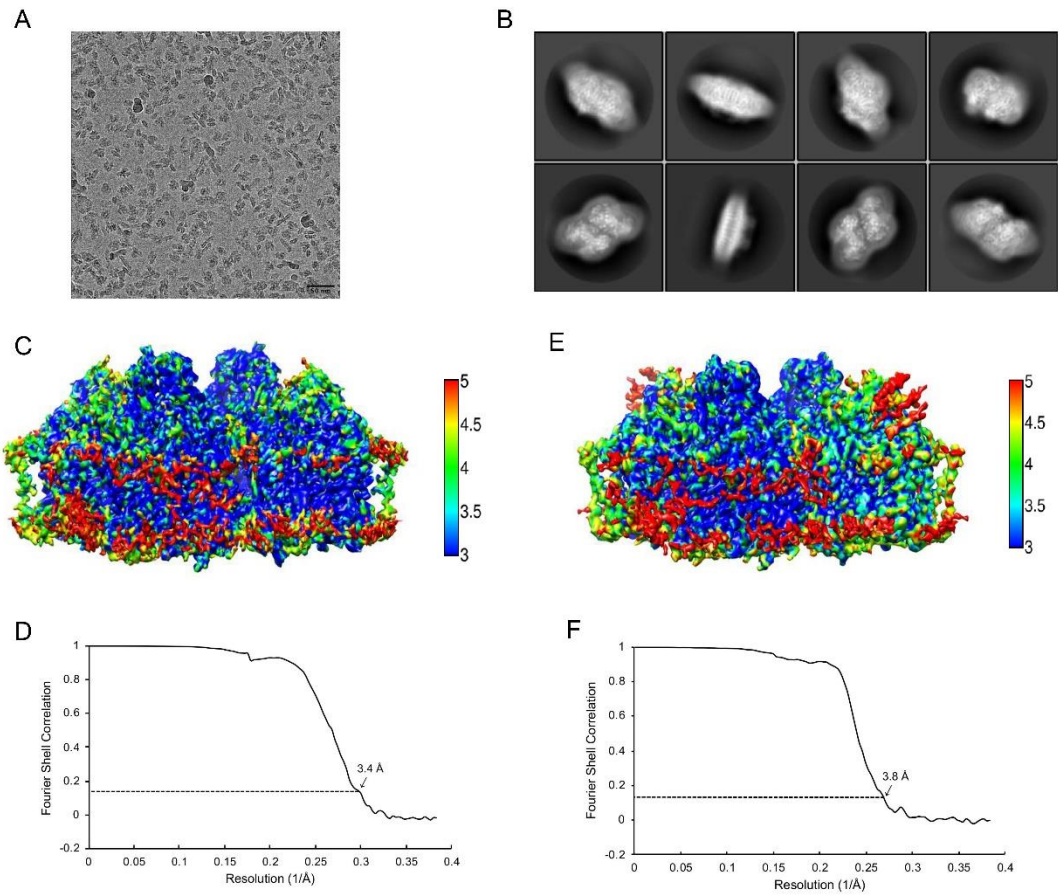

Fig. S3. Cryo-EM images and the cryo-EM map quality. **A:** A representative of cryo-EM micrographs of the Psb27-PSII complex from *T. vulcanus.* **B:** Representatives 2D class average images. **C:** Local resolution distributions of the extrinsic protein depleted PSII complex generated with RELION. **D:** The gold standard FSC curves of the final 3D reconstruction of the extrinsic protein depleted PSII complex. **E:** Local resolution distributions of the Psb27-PSII complex generated with ResMap. **F:** The gold standard FSC curves of the final 3D reconstruction of the Psb27-PSII complex.

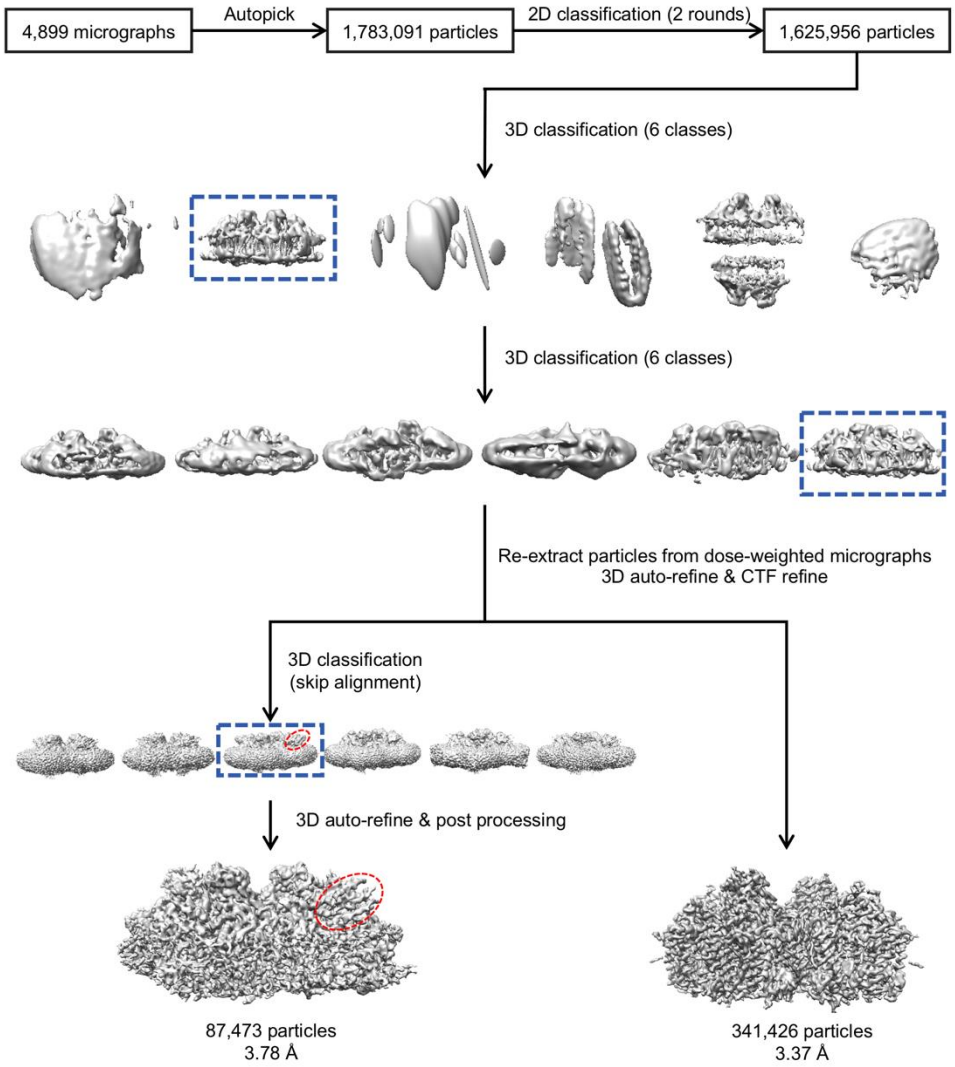

Fig. S4. Flow chart of the cryo-EM data processing. From 4,899 drift-corrected micrographs, 1,783,091 raw particles were picked up and used for 2D classifications. From the results of 2D classifications, 50 classes and 1,625,956 particles were selected for 3D classification which generated 6 classes. The best class was further selected for 3D refinement using *C*1 and then *C*2 symmetry which yielded maps with resolution of 3.78 Å and 3.37 Å, respectively.

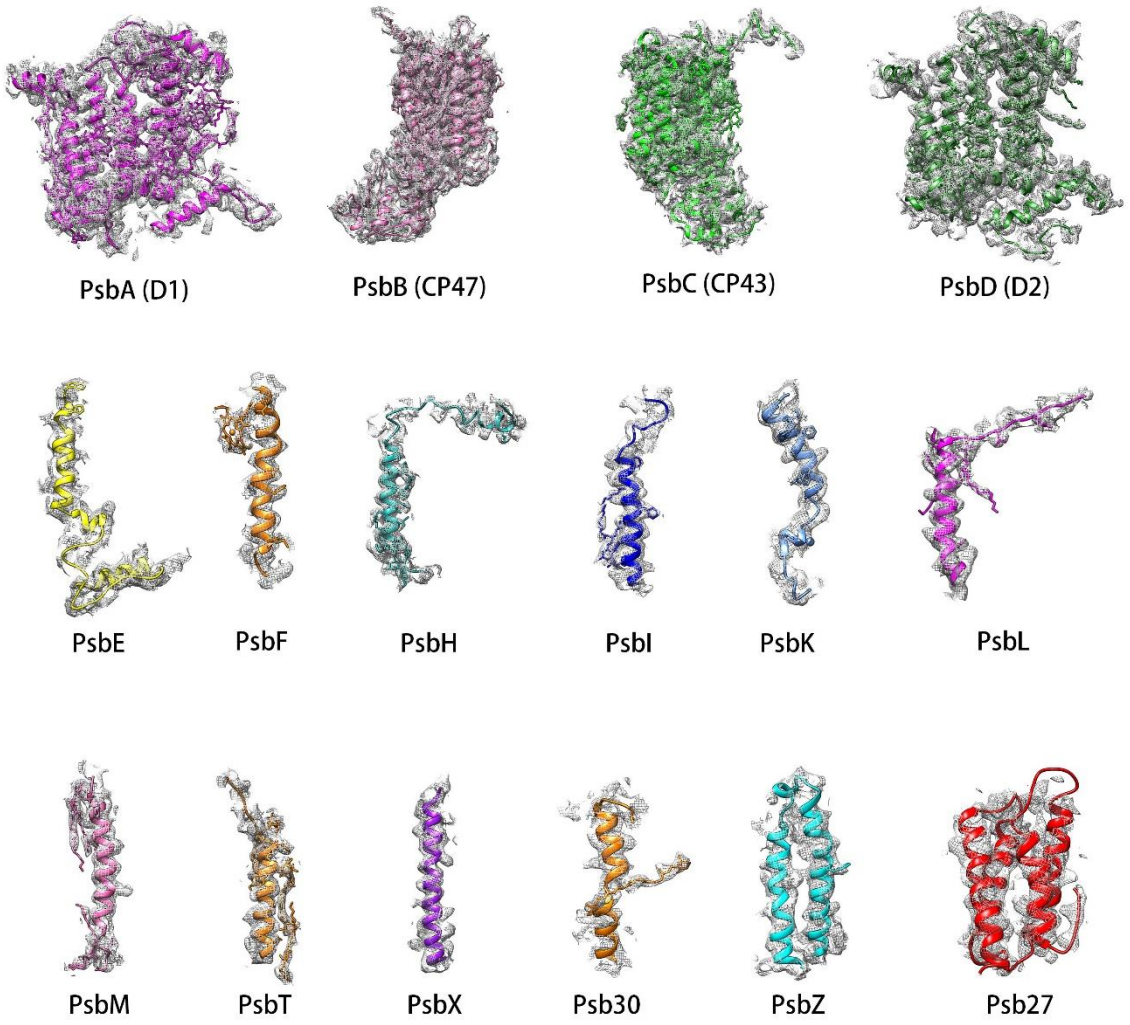

Fig. S5. Cryo-EM densities and structural models of the PSII core intrinsic and extrinsic subunits of the Psb27-PSII complex. The small intrinsic subunits and extrinsic subunit are shown as mixed cartoon/stick model and colored the same as in Fig. 1*C*. The cryo-EM density map of each subunit is depicted in gray meshes. For the trans-membrane subunits, the upper ends represent the cytoplasmic side.

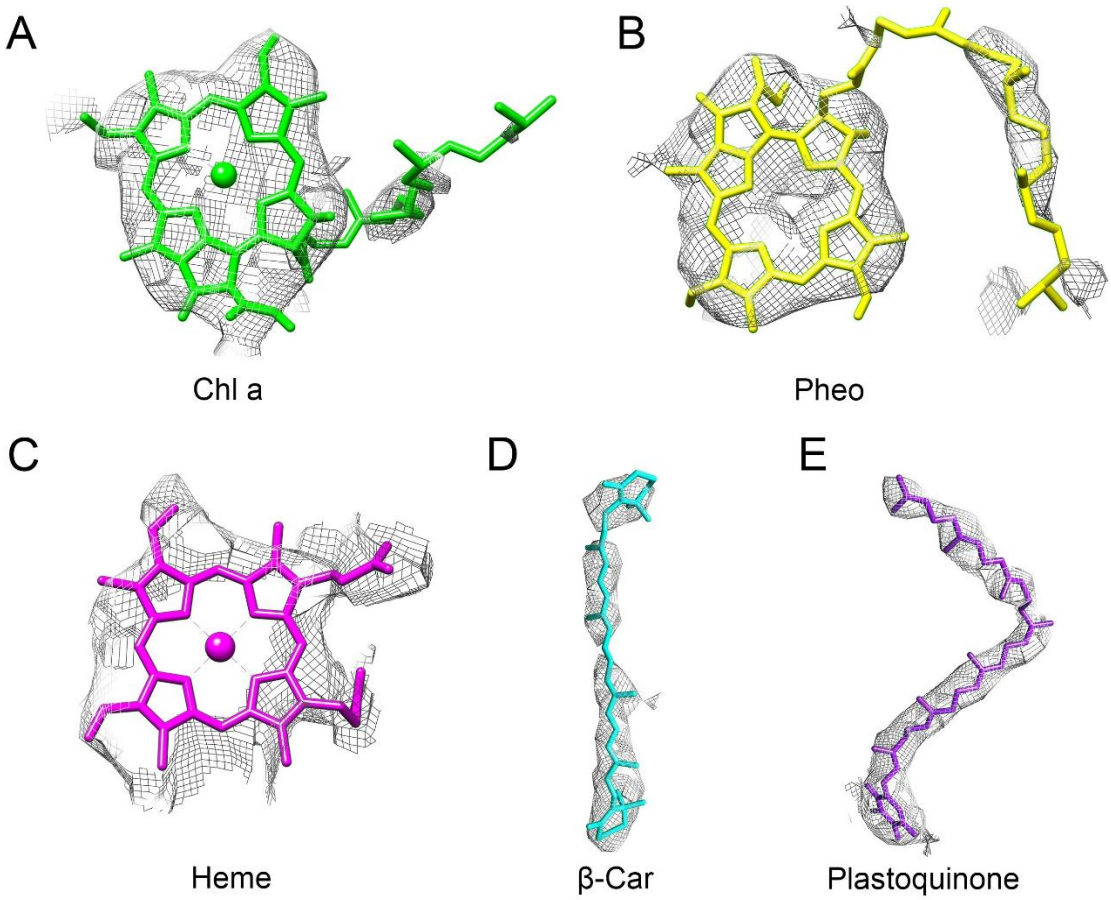

Fig. S6. Cryo-EM densities of various cofactors bound in the Psb27-PSII complex of *T. vulcanus*. The density is shown as gray meshes and all cofactors are shown as stick models. Fe and Mg are shown as purple and green spheres.

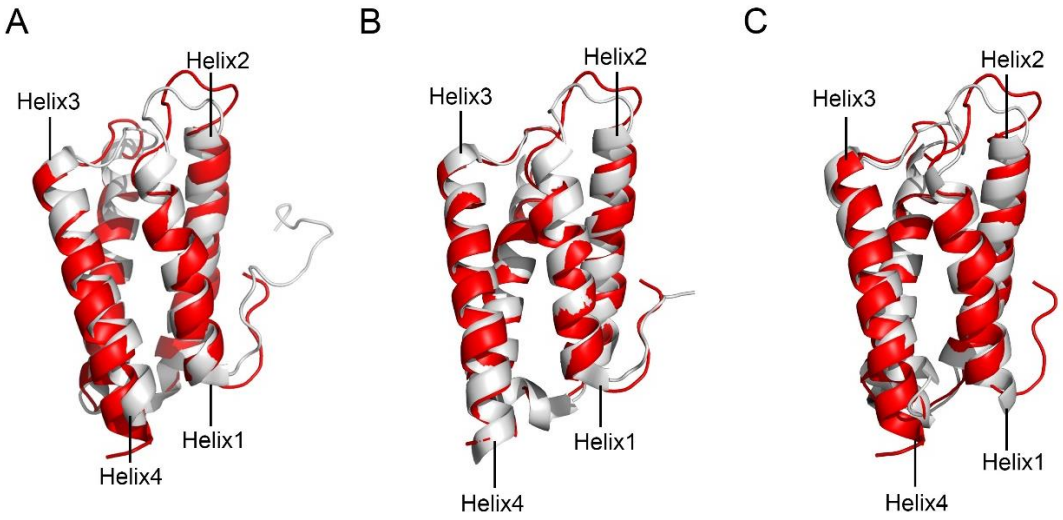

Fig. S7. Structural comparison of the Psb27 subunit from the Psb27-PSII complex of *T. vulcanus* with other recombinant Psb27. **A:** Superposition of the current cryo-EM structure of Psb27 with the NMR structure of Psb27 from *Synechocystis* PCC. 6803 (PDB code: 2KMF). **B:** Superposition of the current cryo-EM structure of Psb27 with the crystal structure of Psb27 from *T. elongatus* (PDB code: 2Y6X). **C:** Superposition of the current cryo-EM structure of Psb27 with the crystal structure of Psb27 from *A. thaliana* (PDB code: 5X56). The Psb27 of *T. vulcanus* is shown in red and Psb27 from other species are depicted in grey.

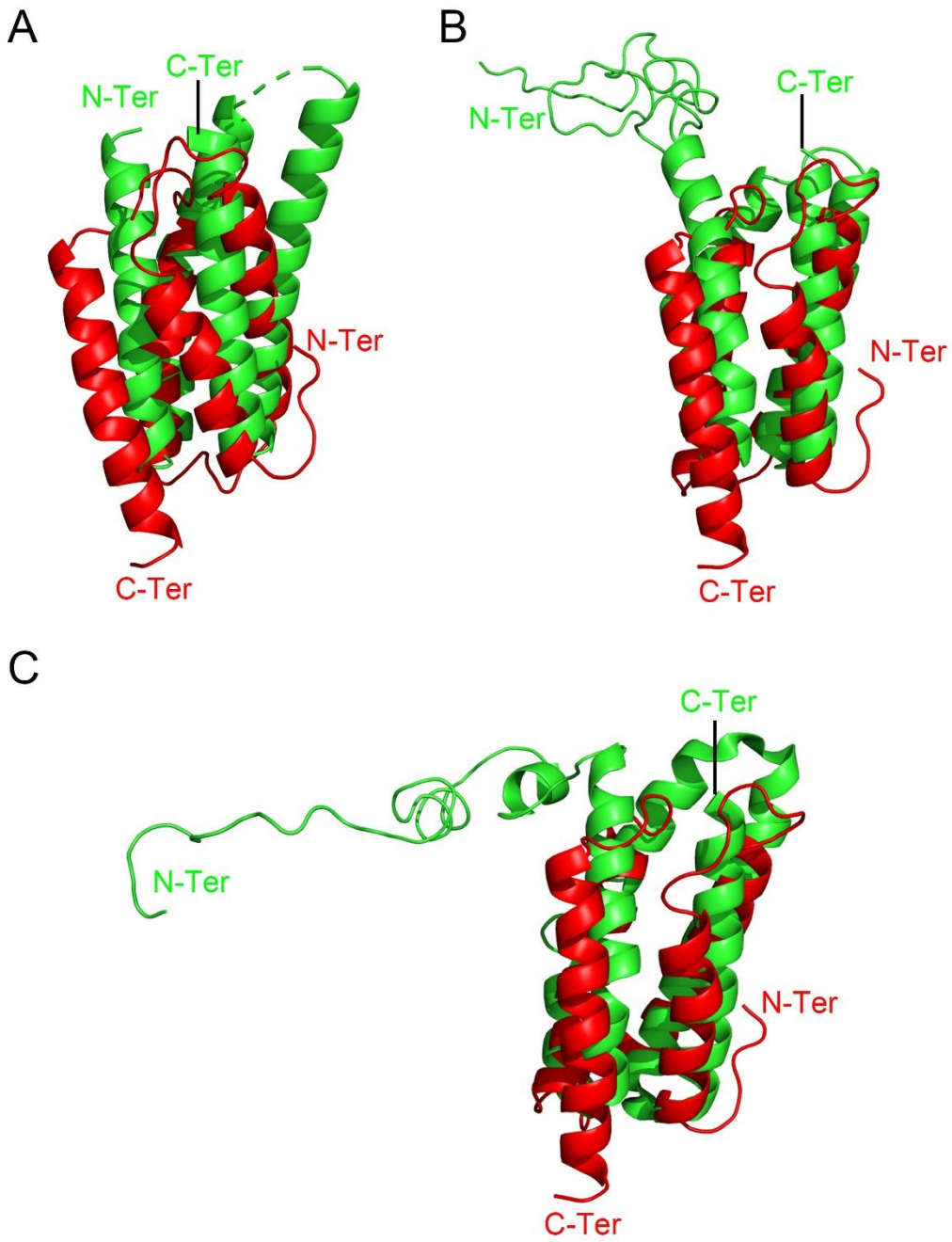

Fig. S8. A close-up view of the positions and orientations of Psb27 in the lumenal side of PSII superimposed with the red algal PsbQ′ (**A**, PDB code: 4YUU), diatom PsbQ′ (**B**, PDB code: 6JLU), and spinach (**C**, PDB code: 3JCU), as shown in Fig.5 *A-C.* Psb27 is shown in red, and PsbQ′ (PsbQ) is shown in green.

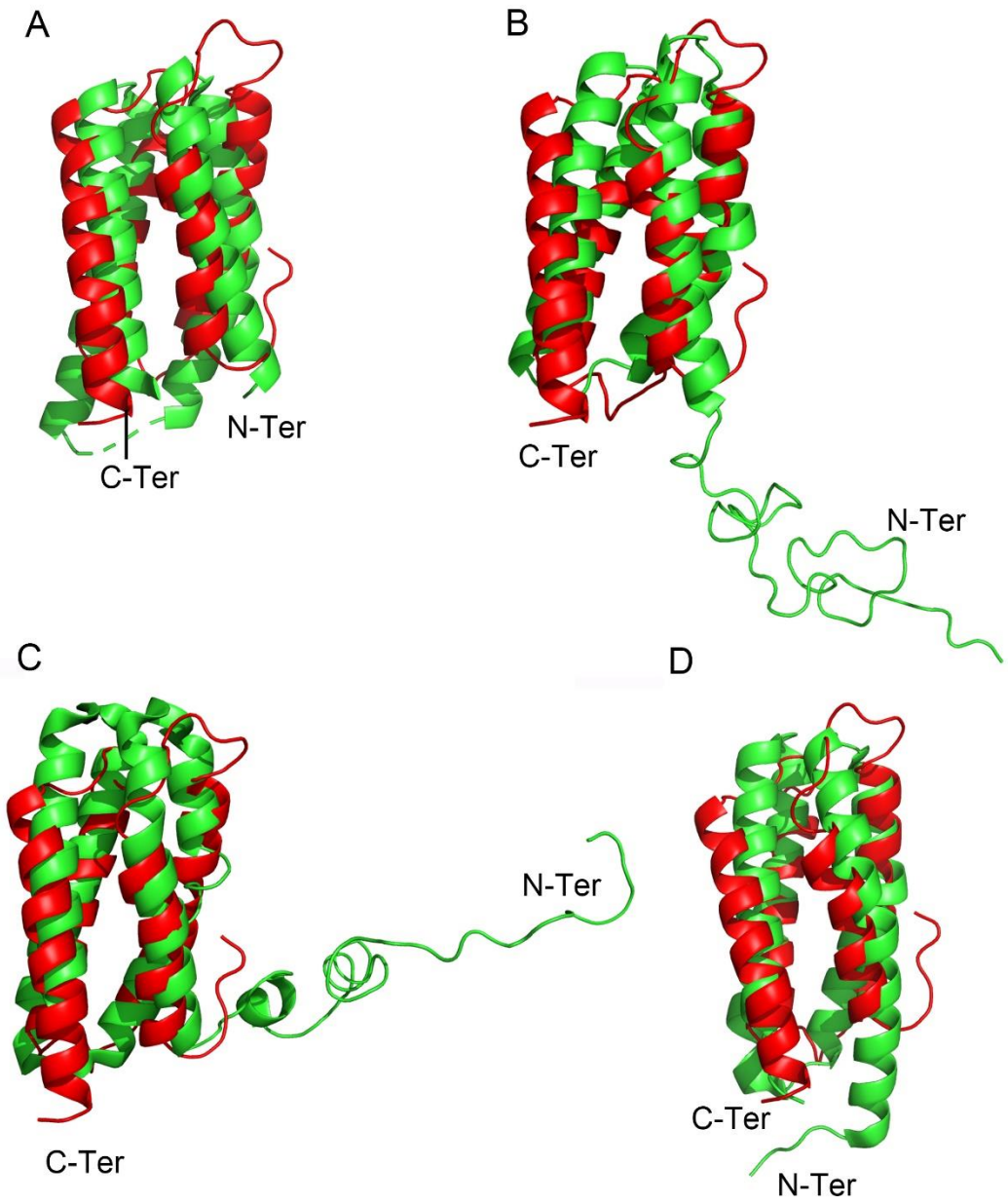

Fig. S9. Structural comparison of Psb27 from *T. vulcanus* with PsbQ or PsbQ′ subunit from other species. **A:** Superposition of structures of Psb27 and CyanoQ of *T. elongatus* (PDB code: 3ZSU). **B:** Superposition of structures of Psb27 and PsbQ′ from a red alga, *C. caldarium* (PDB code: 4YUU). **C:** Superposition of structures of Psb27 and PsbQ′ from a diatom, *C. gracilis* (PDB code: 6JLU). **D:** Superposition of structures of Psb27 and PsbQ from a higher plant, *Spinacia oleracea* (PDB code: 3JCU). The Psb27 is shown in red and PsbQ or PsbQ′ in green. The rmsd values are 3.87, 4.56, 3.83 and 4.11 Å in **A, B, C** and **D**, respectively.

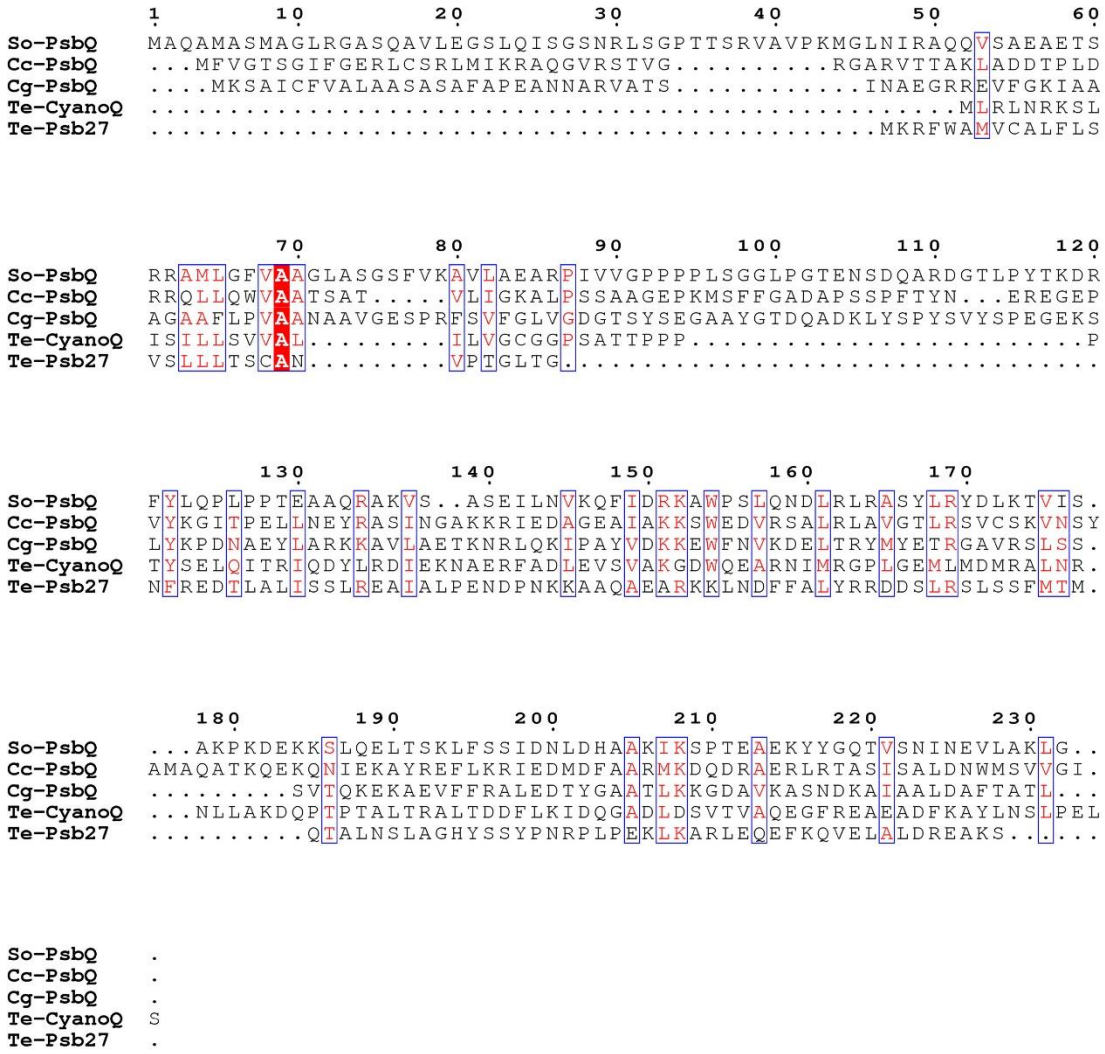

Fig. S10. Sequence alignment of PsbQ, or PsbQ′ from Spinach (*Spinacia oleracea*), a red alga (*C. caldarium*), a diatom (*C. gracilis*), and CyanoQ and Psb27 from a cyanobacterium (*T. elongatus*) (1). Fully conserved residues and similar residues are shaded and shown in red, respectively. All sequences were taken from the National Center for Biotechnology Information (NCBI) database.

Table S1. Cryo-EM data collection, refinement and validation statistics.

Model	PSII core	Psb27-PSII
Data collection and processing		
Magnification	22,500	22,500
Voltage (kV)	300	300
Electron exposure (e^{-}/Å^2)	50	50
Defocus range (μm)	-1.5~-2.5	-1.5~-2.5
Pixel size (Å)	1.30654	1.30654
Symmetry imposed	C2	C2
Initial particle images (no.)	178,3091	178,3091
Final particle images (no.)	341,426	87,473
Map resolution (Å)	3.37	3.78
FSC threshold	0.143	0.143
Refinement		
Number of atoms	38,880	40,602
Protein residues	4,095	4,311
Ligands	146	146
R.m.s. deviations		
Bond lengths (Å)	0.02	0.01
Bond angles (°)	1.57	0.91
Validation		
MolProbity score	2.06	2.38
Clashscore	12.4	24.17
Poor rotamers (%)	0.96	0.12
Ramachandran plot		
Favored (%)	92.84	91.57
Allowed (%)	7.14	8.34
Disallowed (%)	0.02	0.09

Table S2. Cofactors in each subunit of the Psb27-PSII complex assigned in the present study.

Subunit	Traced residues	Chlorophylls	Carotenoids	Lipids	Others
PsbA (D1)	324 (10-333)	4 Chl *a*	1 BCR	2 SQDG	1 Fe ion
		2 Pheo			1 PQ
					1 LMT
					1 LHG
PsbB (CP47)	483 (2-484)	16 Chl *a*	3 BCR		1 MGE
PsbC (CP43)	446 (27-472)	13 Chl *a*	2 BCR	3 DGDG	
PsbD (D2)	339 (13-351)	2 Chl *a*	1 BCR		1 PQ 3 MGE
					1 BCT
PsbE	65 (20-84)				
PsbF	31 (14-44)				1 haem
PsbH	62 (2-63)		1 BCR	1 DGDG	
PsbI	34 (1-34)				1 MGE
					1 FME
PsbK	37 (10-46)		1 BCR		1 CA
PsbL	37 (1-37)			1 SQDG	1 MGE
PsbM	33 (1-33)				1 MGE
					1 LMT
					1 FME
PsbT	30 (1-30)		1 BCR		1 LMT
					1 FME
PsbX	35 (3-37)				
Psb30	29 (18-46)		1 BCR		
PsbZ	62 (1-62)				
Psb27	108 (27-134)				1 Cl

Abbreviations used: BCR, β-carotene; Cl: chloride ion; CA: Calcium ion; Chl *a*: Chiorophyll a; SQDG, sulfoquinovosyldiacyl glycerol; DGDG, digalactosyldiacyl glycerol; BCT: bicarbonate ion; LMT: dodecyl-beta-D-maltoside; LHG: 1,2-dipalmitoyl-phosphatidyl-glycerole; MGE: (1S)-2-(alpha-L-allopyranosyloxy)-1-[(tridecanoyloxy)methyl]ethyl palmitate; FME: N-formylmethionine; Pheo: Pheophytin a; PQ: plastoquinone.

Table S3. Structural changes of the subunits in the dimeric Psb27-PSII complex compared with those in the structure of native PSII (PDB code: 3WU2).

Subunit	Amino acids	Changes	Distance (Å)
PsbA(D1)	61-64	shifted	4.0-4.9
PsbA(D1)	309-311	shifted	2.7-3.2
PsbA(D1)	333	shifted	5.0
PsbA(D1)	334-344	missed	—
PsbB(CP47)	85	shifted	3.5
PsbB(CP47)	350	shifted	3.5
PsbB(CP47)	383-386	shifted	2.3-6.3
PsbB(CP47)	406	shifted	2.9
PsbB(CP47)	490-505	missed	—
PsbC(CP43)	19-26	missed	—
PsbC(CP43)	79	shifted	2.9
PsbC(CP43)	102	shifted	2.7
PsbC(CP43)	212	shifted	2.8
PsbC(CP43)	228	shifted	2.8
PsbC(CP43)	324-327	shifted	2.7-3.4
PsbC(CP43)	334-335	shifted	3.0-3.4
PsbC(CP43)	343-348	shifted	2.9-4.4
PsbC(CP43)	372	shifted	2.7
PsbC(CP43)	381-382	shifted	2.8-3.3
PsbC(CP43)	384-387	shifted	2.7-4.1
PsbC(CP43)	392	shifted	2.8
PsbC(CP43)	396	shifted	2.7
PsbC(CP43)	409-418	shifted	2.7-4.5
PsbD(D2)	352	missed	—
PsbD(D2)	351	shifted	9.3
PsbE	4-19	missed	—
PsbE	20-32	shifted	2.9-4.0
PsbF	12-13	missed	—

Table S4. Hydrogen bonds between the C-terminal residues of D1 subunit and residues from other subunits in the crystal structure of native PSII (PDB code: 3WU2).

	Amino acid residue-1	Amino acid residue-2	Distance (Å)
1	PsbA-Arg334(NE)	PsbO-Pro158(O)	3.0
2	PsbA-Arg334(NH1)	PsbD-Glu312(OE1)	2.9
3	PsbA-Arg334(NH2)	PsbA-Glu65(OE2)	3.0
4	PsbA-Asn335(OD1)	PsbO-Leu157(N)	2.8
5	PsbA-Asn335(ND2)	PsbA-Glu65(OE1)	2.8
6	PsbA-Ala336(N)	PsbA-Glu333(O)	2.9
7	PsbA-His337(O)	PsbD-Asn350(ND2)	2.9
8	PsbA-Asn338(ND2)	PsbC-Lys339(O)	3.2
9	PsbA-Asn338(O)	PsbU-Tyr103(OH)	2.6
10	PsbA-Leu341(O)	PsbC-Gln313(NE2)	2.9
11	PsbA-Leu341(N)	PsbC-Gln313(OE1)	2.9

SI Reference

1. X. Robert, P. Gouet, Deciphering key features in protein structures with the new ENDscript server. *Nucleic. Acids. Res.* **42**, W320-324 (2014).